An algorithm for the generation of biofouled surfaces for applications in marine hydrodynamics

Sotirios Sarakinos and Angela Busse

Abstract The adverse effects of marine biofouling on marine renewable energy devices are well established. In recent fundamental investigations on fluid flow over this type of surface roughness, marine biofouling has mainly been realized as ordered arrangements of roughness elements. These surfaces cannot be compared to realistic biofouled surfaces which show an irregular distribution of roughness features. In this work, a geometric algorithm for generating realistic surface roughness due to barnacle settlement is presented. The algorithm mimics the settlement behaviour of barnacles and allows the generation of a range of fouling states from very sparse rough surfaces to surfaces that are fully covered by barnacle colonies. The generated surfaces can be used in various applications, e.g. in CFD simulations to establish the fluid dynamic roughness effect of different fouling states or as 3D printed surface tiles for use in wind-tunnel and towing tank experiments.

Key words: Roughness, Marine biofouling, Turbulence, DNS, Barnacles, Frictional resistance

1 Introduction

The accumulation of marine organisms on ship hulls or underwater surfaces of man-made structures is collectively defined as marine biofouling. The negative effects these colonies of marine organisms cause can be of economic, environmental, and engineering nature. In 2011 Schultz et al. [21] calculated the economic impact of marine biofouling on naval surface ships and noted that the yearly maintenance and operational costs for a ship can increase by millions of dollars with a small change in

Sotirios Sarakinos
University of Glasgow, Glasgow G12 8QQ, UK. e-mail: sotirios.sarakinos@glasgow.ac.uk

Angela Busse
University of Glasgow, Glasgow G12 8QQ, UK. e-mail: angela.busse@glasgow.ac.uk

their biofouling rating. The increased cost in most cases is a result of the excessive fuel needs, caused by a significant increase in the frictional resistance of submerged surfaces due to biofouling [20]. Loxton et al. [10] reported the effect of marine biofouling on marine renewable energy devices. They stated that biofouling can reduce the energy extraction efficiency of wave or tidal energy harvesting devices, as it can increase the effective diameter of their components, causing an increase in drag and inertia. The need for further study of the effects of biofouling on sea-faring vessels and marine renewable energy devices is apparent.

Marine biofouling can be roughly categorized into microscopic, also known as microfouling, and macroscopic biofouling, also known as macrofouling. The former category encapsulates organisms that are not visible to the naked eye, such as bacteria, diatoms, and protozoa, as well as inorganic matter, such as mud, sand and other materials in particle form [23]. Bacterial organisms and diatoms are responsible for producing a thin film of slime on submerged surfaces. Together with protozoa, rotifers and inorganic material, they form what is known as biofilm. With the term macrofouling all organisms or clusters of organisms are categorized that are large enough to be identified without optical aid. Among the macrofouling organisms the most common ones are barnacles (infraclass *Cirripedia*), mussels, clams and oysters (class *Bivalvia*), tube-worms (family *Serpulidae*), sea-mats (phylum *Bryozoa*), hydroids (class *Hydrozoa*), and sea-squirts (class *Ascidiacea*) [18]. While all macrofouling organisms can be the cause of negative effects, calcareous macrofouling is held accountable for the most severe ones. According to Schultz [19], the increase in frictional resistance of biofouled surfaces escalates when calcareous macrofouling is involved. Although the settlement of marine organisms on submerged surfaces depends heavily on the conditions (temperature, salinity, etc.) of the aquatic environment [22], it is accepted that sessile barnacles (order *Sessilia*), commonly known as acorn barnacles, are among the most dominant calcareous biofouling organisms [3, 12].

Previous research on the effects marine biofouling, either on the hydrodynamic properties of biofouled surfaces, or on the mechanical properties of antifouling coatings, has mainly been focused on experiments performed on plastic or metal plates that were exposed to a biofouling environment for long periods of time [1, 9, 19, 22]. However, such specimens are difficult to obtain, and the settlement of biofouling organisms cannot be easily monitored. The hydrodynamic properties of surfaces with barnacle fouling has been investigated both experimentally and computationally with artificially created surfaces where ordered arrays of barnacle shapes were placed on a flat surface [2, 16], or on an aerofoil element model [14]. However, in reality, barnacles follow an irregular distribution and tend to form clusters. More recently, Demirel et al. [7] performed experiments in a towing tank, using metal plates that were progressively covered with square 3D printed tiles of barnacle clusters. Although the placement of tiles did not follow a typical ordered arrangement, the placement of tiles fully covered by barnacles next to unaffected smooth tiles is not representative of typical barnacle settlement behaviour. In the current work, an algorithm for the generation of more realistic barnacle-type surface roughness is presented. The algorithm mimics the barnacle settlement behaviour to

generate rough surfaces covered by barnacle clusters and allows to create surfaces for a range of fouling states from the onset of fouling to full coverage. The generated surfaces can be used in CFD applications or 3D-printed for use in wind-tunnel or towing tank experiments.

2 Generation of rough surfaces with barnacle shaped roughness elements

Barnacles live their early lives as free swimming larvae (*Nauplii*), that mostly feed on phytoplankton to gather resources, until they metamorphose to *Cyprid* larvae [15]. During their cyprid stage they stop feeding and search for a suitable place to settle. The metamorphosis to a sessile barnacle will confine it to the same spot for the rest of its life, so a place that will provide food, favourable flow conditions, and opportunities for reproduction is required. While there are many factors that govern the barnacle cyprid settlement behaviour, such as surface morphology, existence of light sources and velocity gradient of water current [5], researchers agree [5, 8, 15] that cyprids follow a gregarious behaviour, preferring to settle in places near other already settled barnacles of their own species.

For an algorithm that mimics the barnacle settlement behaviour, the gregarious nature of barnacles had to be captured, as well as the territorial behaviour of cyprids, that would not allow a barnacle shape to be placed within another. Other factors such as light sources, or the initial surface morphology are not included in the current version of the algorithm.

2.1 Definition of the barnacle roughness element

Barnacles reach adulthood when cyprid larvae attach themselves to an underwater surface and become sessile by creating their calcareous outer shell. According to Rainbow [15], sessile barnacle shells consist of a number of interlocking plates ranging from a single plate (e.g *Megatrema anglicum*) to eight (e.g. species of the genus *Catomerus*), based on the evolutionary path that the sessile barnacle species has followed. The shells of most common barnacle species (e.g. *Balanus glandula*, *Semibalanus balanoides*, *Cthamalus stellatus*, *Amphibalanus amphitrite*) consist of six interlocking plates that form a conical frustum-like structure. The barnacle's crustacean body is enclosed inside the shell's mantle cavity and is protected at the upper surface with the paired scuta and terga plates that can be opened and closed as trapdoors (Fig. 1 (left)).

While a living barnacle can move its pair of scuta and terga to feed when submerged, its shell remains static and its shape resembles a conical frustum. Sadique [17] used this kind of geometry to model barnacle shapes and examine the flow around single individuals, or arrays of the same geometry [16]. The barnacle shapes

presented in his work were based on measurements of seven individuals of the *Amphibalanus amphitrite* species. He used their diameter ratio $\frac{2R_1}{2R_2}$, and their aspect ratio $\frac{H}{2R_1}$ to model one frustum with representative size and shape to the seven individuals.

The roughness elements generated in this work are conical frustums, as depicted in Fig. 1 (right), defined similarly to the ones used by Sadique [17]. Every barnacle shape is defined by its lower radius R_1, the upper and lower radii ratio $RR \equiv R_1/R_2$, and its aspect ratio $AR \equiv H/2R_1$. By varying these values, a population of sessile barnacles with a realistic distribution of shape and size can be modelled. To this end, the values of ratios AR and RR are chosen randomly within user defined bounds, allowing for some variation in barnacle shapes, but still ensuring that no barnacle is unnaturally shaped. Given the actual values for the two radii and the frustum height, the height of the frustum at point with distance r from its centre can be calculated as in equation (1)

$$h = \begin{cases} H\dfrac{R_1 - r}{R_1 - R_2}, & R_2 < r \leq R_1 \\ H \qquad\qquad , & r \leq R_2. \end{cases} \tag{1}$$

2.2 Barnacle placement

With the definition of the barnacle geometric characteristics a set of barnacle shapes for fouling of a surface can be modelled. The next task is the placement of barnacles on the smooth reference surface to create realistic barnacle colonies on the final rough surface. The location and occupied space of each barnacle can be defined by their lower radius, and the Cartesian coordinates (x_0, y_0) of their bases' centre, as

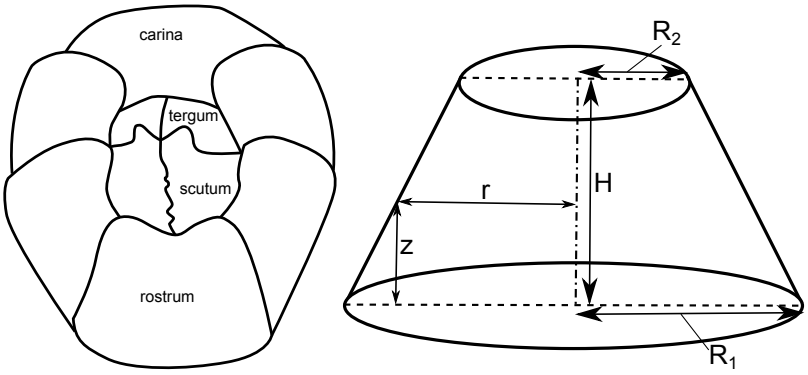

Fig. 1 Sketch of a barnacle with a six-plated shell structure (left), based on sketches of common barnacle species by Rainbow [15]. Frustum representation of barnacle shape (right).

illustrated in Fig. 2. In the following, we assume that barnacles are placed on a flat rectangular reference surface of size $x_{max} \times y_{max}$.

2.2.1 Generic and seed barnacles

As described in section 2, the presented algorithm generates realistic barnacle colonies mainly by reproducing the gregarious behaviour of barnacles when choosing a location to settle. To this end, all barnacles are placed on the reference surface sequentially, while considering already placed barnacles as mature individuals. When a new barnacle is placed, one of the already placed barnacles is randomly chosen as its *neighbour*. The new barnacle will try to settle in the vicinity of this neighbour. The origin of the new barnacle is defined by distance d from the neighbour's centre and angle ϕ as illustrated in Fig. 3 (left). The Cartesian coordinates of the new barnacle's centre can be calculated as in equation (2), where subscript n denotes the neighbour barnacle origin coordinates. Both distance d, and angle ϕ are defined randomly. The bounds of d are controlled by the proximity factor, which is discussed in section 2.2.2, and ϕ is defined within $[0, 2\pi)$. In case the origin of a new barnacle falls without the boundaries of the reference surface, the original choice for the neighbour is discarded and another barnacle is selected as its neighbour

$$\begin{aligned} x_0 &= x_{0_n} + d \cdot \cos\phi \\ y_0 &= y_{0_n} + d \cdot \sin\phi. \end{aligned} \tag{2}$$

The proposed method for placing new barnacle elements on the flat surface requires that at least one initial barnacle shape, i.e. a *seed* barnacle, should already be present. Consequently, the first barnacle will be placed randomly within the boundaries of the empty reference surface as starting point for a barnacle colony. The origin coordinates for the first barnacle are defined within the bounds shown in Eq. 3, to ensure that the whole body of the first barnacle will lie within the surface

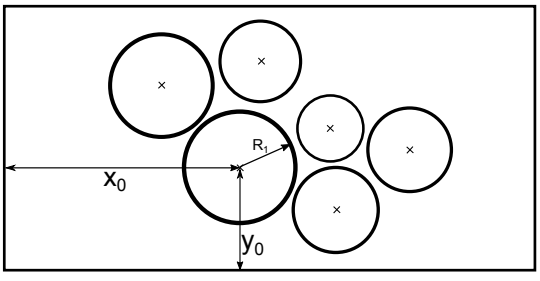

Fig. 2 The location of a barnacle is defined by the Cartesian coordinates of its base centre. The area a barnacle occupies is fully defined by its lower radius.

$$\begin{aligned} x_0 &\in [R_1,\ x_{max} - R_1] \\ y_0 &\in [R_1,\ y_{max} - R_1]\ . \end{aligned} \tag{3}$$

After the first barnacle is placed, the location of the rest of the barnacle shapes can be determined with the proposed methodology. However, if all these shapes are placed within the vicinity of the first barnacle or the ones following, only one barnacle colony will be formed. To enable the formation of several clusters, the number of seed barnacles can be increased. An example of seed barnacle arrangement is presented in Fig. 3 (right). When *generic* barnacles will be added to the surface, seed barnacles will attract them to create clusters.

2.2.2 Regulating barnacle proximity

While the barnacle placement method described in section 2.2 enables the generation of barnacle colonies, with new barnacles settling within the vicinity of already settled mature barnacles, the new barnacle may overlap with other already settled barnacles that are not its selected neighbour. To avoid unwanted overlapping of barnacle shapes when the location of a new barnacle is randomly generated, its distance from all the existing barnacles is checked. The minimum allowed distance of the new barnacle from all existing barnacles is defined with the use of a proximity factor $f_p > 0$ that is used as shown in equation (4), where subscripts e and s denote any already existing barnacle and the new settling barnacle, respectively, while O is their origin

$$|\mathbf{O_e O_s}| \geq f_p \cdot (R_{1_e} + R_{1_s}). \tag{4}$$

When placing a barnacle, the distance d from its selected neighbour is set to a value $d > f_p(R_{1_n} + R_{1_s})$, so that the proximity criterion is fulfilled with respect to the selected neighbour. To ensure that the proximity criterion is also fulfilled with respect to all other existing barnacles, equation (4) is evaluated for these before settling the new one. If the proximity check fails for any settled barnacle, the original neighbour is discarded and a new neighbour is selected among the existing barnacles,

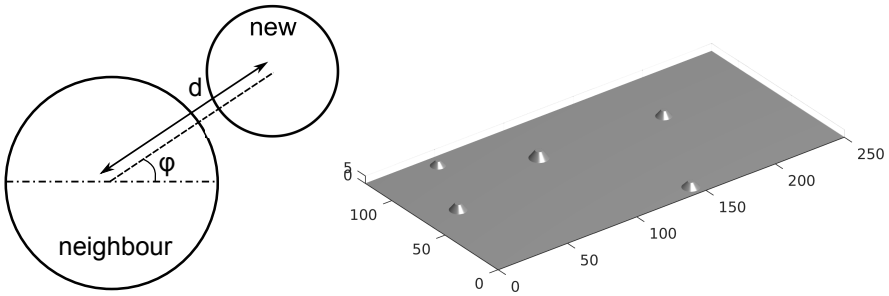

Fig. 3 Positioning a new generic barnacle with respect to its neighbour (left). Distribution of seed barnacles that will attract generic ones (right). Dimensions in mm.

and the proximity check is repeated. After a large number of failed attempts to settle, the new barnacle is not placed on the surface, and the algorithm terminates. This part of the settling methodology was inspired by the barnacle cyprid walk and territorial behaviour [15].

The value of f_p controls the density of barnacle clusters. With $0 < f_p < 1$, overlapping of barnacles is allowed and tightly packed barnacle colonies are generated. When $f_p = 1$ barnacles are allowed to touch, while with $f_p > 1$ no touching is allowed and loosely packed colonies are generated. The effect of f_p can be observed in Fig. 4, where three surfaces with the same number of barnacles, but different values of f_p are illustrated. The proximity check is used for the placement of all barnacles apart from the first one, although different values are used for seed and generic barnacles, so that seed barnacles can be more widespread resulting in more distinct barnacle clusters. Although random values of the proximity factor can also be used, in this work the proximity factors for seed and generic type barnacles are fixed for that specific barnacle type.

2.2.3 Resolving periodicity

When generating rough surfaces for CFD simulations or for tiling of wind-tunnel floors it is often necessary for the surface to be periodic in one or both horizontal directions. Periodicity can be enforced in the current surface roughness generation algorithm by a simple modification: When a barnacle's origin is positioned at a distance less than its radius from the edges of the flat plate, the portion of its geometry that exceeds the surface boundaries must be copied to the opposite periodic

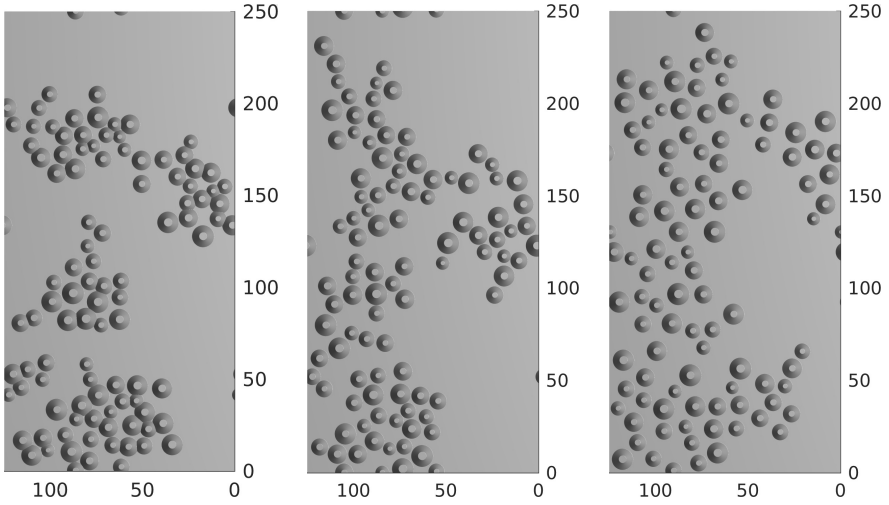

Fig. 4 Barnacle covered surfaces containing the same number of barnacles, generated with proximity factors $f_p = 0.8$ (left), $f_p = 1$ (middle), and $f_p = 1.1$ (right). Dimensions in mm.

position. In case the new barnacle is placed near one of the corners of the flat rectangular surface, portions of the barnacle need to be copied to the three other corners. Examples of periodic barnacles are illustrated in Fig. 5. When periodicity is included, proximity of a new barnacle to existing ones needs to be calculated taking into account the periodic boundaries.

2.3 The barnacle placement algorithm

Combining the information presented in Sects. 2.1 and 2.2, the algorithm for generating rough surfaces is described below:

1. Define the number of *generic* and *seed* barnacles to be placed.
2. Randomly generate the geometric characteristics for all barnacles (R_1,RR,AR) and select the desired number of seed barnacles.
3. For all seed barnacles:
   a. Randomly generate coordinates of origin within the reference surface boundaries.
   b. Check that the proximity constraint (see equation (4)) applies for proximity factor f_p^{seed}.
4. For all remaining generic barnacles:
   a. Pick one of the already placed barnacles as *neighbour*.
   b. Randomly generate parameters d and ϕ (see Fig. 3), and calculate the new barnacle's origin coordinates.
   c. Check that the proximity constraint applies for the proximity factor $f_p^{generic}$. If the proximity constraint is not satisfied, go to step 4a.
   d. Apply periodicity if required.
5. The algorithm ends when all barnacles have been placed on the surface, or when the proximity check in step 4c fails too many times, which means that there is not enough space left to place another barnacle.

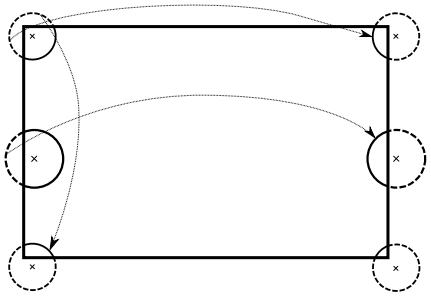

Fig. 5 Periodicity can be imposed by copying exceeding parts of barnacles to the opposite sides of the flat surface. Special care has to be taken when the barnacle is settled close to a corner of the surface and different parts have to be copied to different surface sides.

3 Application

The rough surfaces generated with the proposed algorithm can be used in various applications involving the investigation of fluid flows over surfaces fouled with barnacles, both experimentally and in CFD. As an example, the barnacle covered surface illustrated in Fig. 6 has been used as a rough wall in a DNS of turbulent channel flow to establish its effect on near-wall turbulence using an embedded boundary approach [4]. The rough surface consists of 275 barnacles, eight of which were seed barnacles. Generic barnacles were placed with a proximity factor $f_p^{generic} = 0.8$, while $f_p^{seed} = 4$ was used for seed ones. The initial size of the rectangular flat surface was $250 \times 125 mm^2$, and the lower radius R_1 of all barnacles was randomly defined within $[3.5, 6]mm$. Ratios RR and AR were defined within $[0.31, 0.4]$ and $[0.34, 0.42]$, respectively, based on measurements by Sadique [17], and d was bounded within $[0.8, 1.2](R_{1_s} + R_{1_n})$. For use in the DNS, the rough surface was non-dimensionalised with the mean channel half-height δ as reference. The size of the computational domain was $2\pi\delta \times \pi\delta$ in the streamwise and spanwise directions, while the largest barnacle height was 0.1267δ. The simulation was performed at $Re_\tau = 395$ at a grid resolution of $864 \times 432 \times 512$ with uniform spacing in the streamwise and spanwise directions ($\Delta x^+ = \Delta y^+ = 2.8$). The spacing in the wall-normal direction is uniform up to the maximum roughness height with $\Delta z^+_{min} = 0.667$, and stretched above, reaching $\Delta z^+_{max} = 3.11$ at the channel centre.

The Hama roughness function ΔU^+ is defined as the downward shift of mean streamwise velocity profile compared to the equivalent of the flow over a smooth surface. The current simulation provided a roughness function value of $\Delta U^+ \approx 7.95$ characterizing the flow in the fully rough regime according to Nikuradse [13]. The equivalent sand-grain roughness of this surface can then approximated to be $k_{s,eqv} \approx 1.8 k_{max}$, where k_{max} is the maximum peak-to-valley height of the rough surface, which coincides with the maximum barnacle height. Vortex identification with the Q-criterion (see Fig. 6 (right)) illustrates how the flow between the roughness elements can be investigated using this kind of simulations.

Although the proposed algorithm has been been introduced in the context of a flat rectangular reference surface, it can be implemented for other types of reference surfaces as well, such as curved surfaces within an hydrofoil design. Taking into

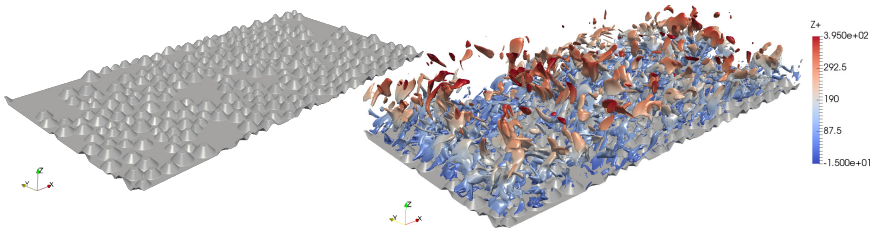

Fig. 6 Rough surface with 60% barnacle coverage (left) was used as boundary condition in DNS of turbulent channel flow. Instantaneous vortices are identified with the Q-criterion (Q=15000) (right).

account that the barnacle location and area is defined by its base origin and its lower radius, the barnacle bases could be projected on a curved surface allowing the remaining steps of the algorithm to proceed as described above.

4 Conclusion

In this work an algorithm for the generation of barnacle fouled rough surfaces has been presented. The proposed methodology mimics the settlement behaviour of barnacles, resulting in realistic examples of surfaces covered with barnacle clusters. The number of barnacle clusters can be controlled by adjusting the number of generic and seed barnacles that are placed on the surface, while the barnacle arrangement can be regulated by a proximity factor that controls how close new barnacles will be placed to already settled ones. As an example, a rough surface with 60% barnacle coverage has been used in DNS of rough-wall turbulent channel, giving the equivalent sand-grain roughness of the surface, and allowing a detailed investigation of changes in near-wall turbulence induced by this type of marine biofouling.

Acknowledgements This work was supported by the Engineering and Physical Sciences Research Council (EPSRC) [grant number EP/P009875/1].

References

1. Andrewartha J, Perkins K, Sagrison J, Osborn J, Walker G, Henderson A, Hallegraeff G (2010) Drag forces and surface roughness measurments on freshwater biofouled surfaces. Biofouling 26(4):487–496
2. Barros J M, Murphy E A, Schultz M P (2016) Particle image velocimetry measurements of the flow over barnacles in a turbulent boundary layer. In Proceedings of the 18th International Symposium on the Application of Laser and Imaging Techniques to Fluid Mechanics
3. Berntsson K M, Jonsson P R (2003) Temporal and spatial patterns in recruitment and succession of a temperate marine fouling assemblage: a comparison of static panels and boat hulls during the boating season. Biofouling 19(3):187–195
4. Busse A, Lützner M, Sandham N D (2015) Direct numerical simulation of turbulent flow over a rough surface based on a surface scan. Comput Fluids 116:129–147
5. Crisp D J (1955) The behaviour of barnacle cyprids in relation to water movement over a surface. J Exp Biol 32(3):569–590
6. Crisp D J (1961) Territorial behaviour in barnacle settlement. J Exp Biol 38:429–446
7. Demirel Y K, Uzun D, Zhang Y, Fang H-C, Day A H, Turan O (2017) Effect of barnacle fouling on ship resistance and powering. Biofouling 33(10):819–834
8. Knight-Jones E W, Crisp D J (1953) Gregariousness in barnacles in relation to the fouling of ships and to anti-fouling research. Nature 171:1109–1110
9. Lindholdt A, Dam-Johansen K, Olsen S M, Yebra D M, Kiil S (2015) Effects of biofouling development on drag forces of hull coatings for ocean-going ships: a review. J Coat Technol Res 12(3):415–444
10. Loxton J, Macleod A K, Nall C R, McCollin T, Machado I, Simas T, Vance T, Kenny C, Want A, Miller R G (2017) Setting an agenda for biofouling research for the marine renewable energy industry. Int J of Mar Energy 19:292–303

11. Mullineaux L S, Butman C A (1991) Initial contact, exploration and attachment of barnacle (Balanus amphitrite) cyprids settling in flow. Mar Biol 110:93–103
12. de Messano L V R, Sathler L, Reznik L Y, Coutinho R (2009) The effect of biofouling on localized corrosion of the stainless steels N08904 and UNS S32760. Int Biodeterior Biodegrad 63:607–614
13. Nikuradse J (1933) Strömungsgesetze in rauhen Rohren. VDI Forschungsheft 361
14. Orme J A C, Masters I, Griffiths R T (2001) Investigation of the effect of biofouling on the efficiency of marine current turbines. In French C (ed.), Proc. MAREC 2001:91–99
15. Rainbow P S, An introduction to the biology of British littoral barnacles. Field Stud 6:1-51
16. Sadique J, Yang X I, Meneveau C, Mittal R (2015) Simulation of boundary layer flows over biofouled surfaces. In Proceedings of the 22nd AIAA Computational Fluid Dynamics Conference (AIAA 2015-2616)
17. Sadique J (2016) Turbulent flows over macro-scale roughness elements - From biofouling barnacles to urban canopies. John Hopkins University, Baltimore, Maryland
18. Salta M, Chambers L, Wharton J, Wood R, Briand J F, Blache Y, Stokes K R (2009) Marine fouling organisms and their use in antifouling bioassays. In Proceedings of the European Corrosion Congress (EUROCORR) 2009
19. Schultz M P (2004) Frictional resistance of antifouling coating systems. J Fluids Eng 126:1039–1047
20. Schultz M P (2007) Effects of coating roughness and biofouling on ship resistance and powering. Biofouling 23(5):331–341
21. Schultz M P, Bendick J A, Holm H R, Hertel W M (2011) Economic impact of barnacle fouling on a naval surface ship. Biofouling 27(1):87–89
22. Vance T R, Fileman T (2014) ETI MA1001 - Reliable data acquisition platform for Tidal (ReDAPT) project: ME8.5 "Final Report". Energy Technologies Institute, UK
23. Woods Hole Oceanographic Institution (1952) Marine biofouling and its prevention. U.S. Naval Institute, Annapolis, Maryland